Neuron
Article

Active Dendritic Conductances Dynamically Regulate GABA Release from Thalamic Interneurons

Claudio Acuna-Goycolea,[1] Stephan D. Brenowitz,[1] and Wade G. Regehr[1,*]
[1]Department of Neurobiology, Harvard Medical School, Boston, MA 02115, USA
*Correspondence: wade_regehr@hms.harvard.edu
DOI 10.1016/j.neuron.2007.12.022

SUMMARY

Inhibitory interneurons in the dorsal lateral geniculate nucleus (dLGN) process visual information by precisely controlling spike timing and by refining the receptive fields of thalamocortical (TC) neurons. Previous studies indicate that dLGN interneurons inhibit TC neurons by releasing GABA from both axons and dendrites. However, the mechanisms controlling GABA release are poorly understood. Here, using simultaneous whole-cell recordings from interneurons and TC neurons and two-photon calcium imaging, we find that synchronous activation of multiple retinal ganglion cells (RGCs) triggers sodium spikes that propagate throughout interneuron axons and dendrites, and calcium spikes that invade dendrites but not axons. These distinct modes of interneuron firing can trigger both a rapid and a sustained component of inhibition onto TC neurons. Our studies suggest that active conductances make LGN interneurons flexible circuit-elements that can shift their spatial and temporal properties of GABA release in response to coincident activation of functionally related subsets of RGCs.

INTRODUCTION

Inhibitory interneurons play crucial computational roles in many brain regions (Callaway, 2004; Cruikshank et al., 2007; Gabernet et al., 2005; Guillery and Sherman, 2002; Murphy et al., 2005; Pouille and Scanziani, 2001, 2004; Silberberg and Markram, 2007). In thalamic dorsal lateral geniculate nucleus (dLGN), interneurons are thought to shape information flow from the retina to the cortex (Norton and Godwin, 1992; Sherman, 2004). Visual sensory information is conveyed from retinal ganglion cells (RGC) to thalamocortical (TC) neurons in the dLGN, which in turn project their axons to the visual cortex (Hubel and Wiesel, 1979). Within the dLGN, TC cell activity is modulated by feedforward inhibition provided by local GABAergic interneurons. dLGN interneurons are activated by RGCs and provide feedforward inhibition onto TC neurons (Guillery and Sherman, 2002). These interneurons are thought to refine the receptive fields of TC cells by enhancing surround inhibition (Norton and Godwin, 1992; Norton et al., 1989; Sillito and Kemp, 1983). Inhibitory interneurons may also control the number of visually evoked spikes in TC neurons and the precision of their timing (Berardi and Morrone, 1984; Blitz and Regehr, 2005; Usrey and Reid, 1999).

Although dLGN interneurons have several intriguing properties, the manner in which they provide inhibition is not well understood. One important feature of interneurons is that they contain GABAergic vesicles in their dendrites (Famiglietti, 1970; Famiglietti and Peters, 1972; Montero, 1986). These vesicles have been observed within terminal dendritic protrusions or in bouton-like structures along main dendritic shafts (Hamos et al., 1985; Rafols and Valverde, 1973). Interneuron dendritic specializations are known to establish synaptic contacts with postsynaptic TC neurons (Hamos et al., 1985; Rafols and Valverde, 1973). It has therefore been suggested that, in addition to conventional transmitter release from the axon, interneurons can release GABA from their dendrites. However, the fundamental mechanisms by which RGC activation triggers GABA release from interneuron dendrites and axons are not known. Of particular interest is whether action potentials invade the dendrites of interneurons and thereby control dendritic GABA release (Cox et al., 1998; Crunelli et al., 1988; Sherman, 2004).

In this study, we evaluate the impact of active interneuron firing on the spatial and temporal properties of dendritic and axonal transmitter release. We find that sodium and calcium conductances, which can be activated by synchronous firing of groups of RGCs, allow interneurons to dynamically release GABA from dendrites and axons with distinct temporal properties.

RESULTS

RGC Activation Can Evoke Sodium and Calcium Spikes in LGN Interneurons

We first investigated the functional properties of interneurons that could influence dendritic release. Whole-cell recordings were obtained from interneurons (Figure 1A) identified by GFP expression (Marowsky et al., 2005; Tamamaki et al., 2003), and RGC inputs were stimulated with an extracellular electrode placed in the optic tract around 1 mm away from recorded cells. Under our experimental conditions, RGC-interneuron transmission was mediated by activation of both AMPA and NMDA receptors (n = 35, data not shown). Optic tract stimulation evoked either a single action potential (Figure 1B, left), a prolonged plateau potential (Figure 1B, right in red), or multiple action potentials riding on a depolarizing plateau potential (Figure 1B, right in black) (Zhu et al., 1999). Single spikes or bursts could also be induced by brief somatic depolarization (Figure 1C, top).

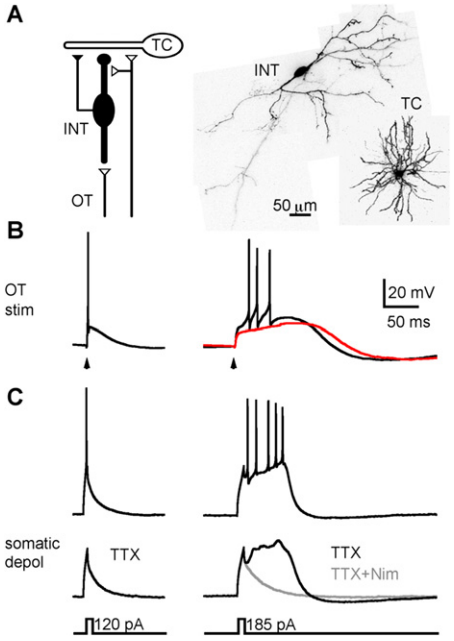

Figure 1. LGN Interneurons Fire Both Sodium and Calcium Spikes

(A) (Left) Schematic of an LGN microcircuit in which RGC axons excite thalamocortical cells (TC) and interneurons (INT) that in turn inhibit TC neurons via dendritic (filled circle) and axonal (filled triangle) synapses. (Right) Inverted fluorescence images taken with a two-photon microscope show interneuron and TC cell morphology.

(B) Firing patterns in a representative interneuron after optic tract (OT) stimulation (arrowhead, 60 μA for 300 μs).

(C) Somatic current injection (10 ms) evoked either a single TTX-sensitive spike (left) or a burst of TTX-sensitive spikes riding on a calcium spike (right) that was blocked by nimodipine (gray).

Resting membrane potentials were (in mV) −63 for (B), −60 for (C).

The blockade of voltage-gated sodium channels with TTX (0.5 μM) eliminated fast action potentials (Figure 1C, bottom left, n = 17). Depolarizing plateau potentials were TTX resistant and abolished by blocking L-type calcium channels with nimodipine (10 μM) (Figure 1C, lower right, gray, n = 12). Thus, LGN interneurons can fire both sodium and calcium spikes.

Active Interneuron Firing Evokes Widespread Intradendritic Calcium Elevations

Previous studies have established that action potentials can invade the dendrites of many types of neurons (Goldberg and Yuste, 2005; Waters et al., 2005), but it is not known whether the calcium and sodium action potentials observed in somatic recordings of LGN interneurons invade the dendrites and thereby contribute to GABA release. Thus, determining the spatial profile of intradendritic calcium increases evoked by either sodium or calcium spikes in LGN interneurons may provide insight into the extent of dendrodendritic synapses activated by these firing modes. We therefore determined the spatial features of calcium elevations evoked by active interneuron firing using two-photon laser scanning microscopy (Denk et al., 1990; Svoboda and Yasuda, 2006). Recordings were made with a pipette containing the red dye Alexa 594 (50 μM) to visualize cells and the green calcium indicator fluo-5F (100 μM). Single action potentials were triggered by 5 ms pulses of somatic current injection, and calcium levels were monitored in dendrites and axons in line-scan mode (Brenowitz et al., 2006). As expected, single spikes evoked calcium signals in axonal boutons, and these signals were completely eliminated by bath application of 0.5 μM TTX (Figures 2A–2D, red, 13 neurons). In dendrites, calcium elevations were monitored in structures along main interneuron dendritic shafts and in dendritic protrusions. As these structures have been shown to contain synaptic vesicles filled with GABA (Famiglietti and Peters, 1972; Montero, 1986; Rafols and Valverde, 1973; Ralston, 1971), calcium elevations triggered here by active interneuron firing may lead to GABA release. Sodium action potentials consistently evoked fast, TTX-sensitive calcium increases in these dendritic specializations (Figures 2A–2C, blue, n = 98). A single sodium spike increased dendritic calcium by 63 ± 7 nM (n = 35). To determine whether these calcium signals attenuate with distance from the soma, we studied calcium levels in dendritic structures located up to 320 μm away from the cell body. As shown in Figure 2D, calcium transients triggered by somatic sodium spikes did not attenuate with distance from the soma (n = 84). Thus, sodium action potentials evoke widespread calcium signals in LGN interneurons, further suggesting that they may evoke GABA release throughout dendrites and axons.

In parallel experiments, we studied dendritic and axonal calcium signals evoked by calcium spikes in interneurons. Calcium spikes were typically triggered by somatic injection of positive current in the presence of TTX (Figure 2 and Figure S1 available online). Interneuron calcium spikes elevated calcium throughout the dendritic arbor (Figures 2E–2G, n = 77) and showed no significant attenuation with distance from the soma (Figure 2H, n = 48). Calcium increases evoked by calcium spikes were larger (740 ± 100 nM, n = 27) and slower (200–300 ms time to peak) compared to those induced by sodium spikes. In a subset of experiments, we tested the effect of the L-type calcium channel antagonist nimodipine on these calcium transients. Nimodipine reduced them by 85% ± 10% (n = 18, data not shown), indicating that they were mainly mediated by activation of dendritic L-type calcium channels.

We then triggered calcium spikes in the soma and measured calcium signals in putative boutons of LGN interneuron axons. In proximal axons (<50 μm), calcium spikes sometimes evoked modest calcium increases (Figures S1A–S1C, red). These small and slow calcium transients may reflect activation of a small fraction of voltage-gated calcium channels due to passive spread of electrical signals from somatic compartments. Alternatively, they may reflect passive diffusion of calcium ions from the soma. In contrast to dendrites, no calcium signals were detected in axons located more than 50 μm from the soma (Figures S1A and S1D, red, n = 35), further establishing that calcium spikes propagated throughout dendrites but not axons. Together, these results suggest that calcium spikes may evoke widespread dendritic GABA release without affecting axonal signaling.

Timing of Inhibition Mediated by Sodium and Calcium Spikes

We used paired recordings from LGN interneurons and TC cells to investigate the contribution of sodium and calcium spikes to

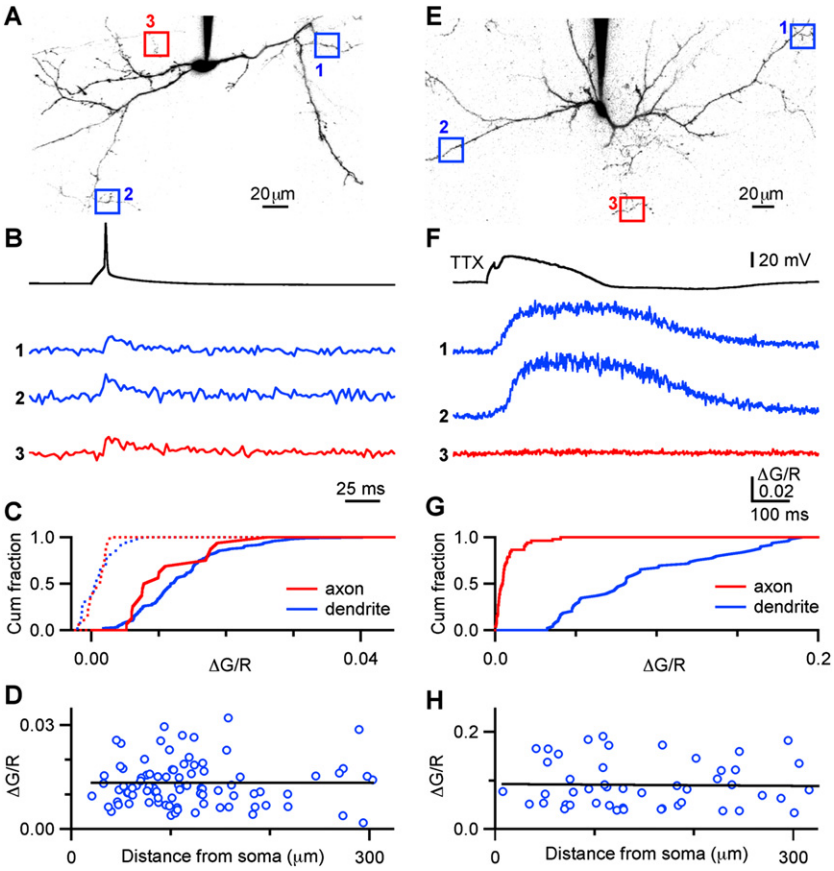

Figure 2. Sodium and Calcium Spikes Elevate Calcium Levels throughout Interneuron Dendrites

Calcium signals evoked by somatic depolarization were measured after single sodium spikes (A–D) or calcium spikes evoked in TTX (E–H). (A and E) Images of interneurons with dendritic (blue) and axonal (red) areas selected for imaging. (B and F) Calcium transients evoked by a sodium spike (B) (top) or a calcium spike (F) (top) were measured in the dendrites (blue traces) and axon (red traces). Cumulative distributions are shown for the amplitudes of calcium transients (ΔG/R) for sodium spikes (C) and for calcium spikes (G). The effect of TTX on calcium elevations evoked by sodium spikes is shown (C) (dotted lines). (D and H) Amplitudes of dendritic calcium elevations (ΔG/R, blue open circles) plotted against distance from the soma were fitted by a linear function (black lines), with slopes for (D) and (H) of −7e−08 ± 1e−05 μm^{-1} and −1e−05 ± 8e−05 μm^{-1}, respectively. Resting membrane potentials were (in mV) −60 for (B) and −62 for (F).

GABA release (Figure 3A). In some trials, prolonged interneuron depolarization could evoke either fast or slow active responses (Figure 3B, left, upper traces) that led to correspondingly fast or slow GABAergic currents (Figure 3B, left, lower traces). In other trials, interneuron stimulation triggered slow active responses that triggered fast presynaptic action potentials (Figure 3B, right, upper red trace) and evoked both slow and rapid GABAergic currents in postsynaptic TC cells (Figure 3B, right, lower red trace). These recordings illustrate that complex active responses in individual LGN interneurons, consisting of a combination of sodium and calcium spikes, control the amplitude and time course of inhibitory currents recorded in TC neurons.

We then directly examined the properties of interneuron-TC synapses when transmission was triggered by either a sodium spike (Figures 3C and 3E) or a calcium spike (Figures 3D and 3F) in isolation. Sodium spikes were evoked in interneurons by brief depolarizing current pulses (50–200 pA for 5–10 ms), and inhibitory currents were recorded in TC cells voltage clamped at +10 mV [$E_{(Cl^-)}$ = −40 mV]. Presynaptic action potentials triggered fast (10%–90% rise time, t_{10-90} of 1.2 ms) TTX-sensitive IPSCs in the postsynaptic cell (Figure 3C). These currents were eliminated by 20 μM picrotoxin and therefore were dependent on the activation of $GABA_A$ receptor type located in TC cell dendrites (n = 7, data not shown). Whether this form of fast inhibition results from GABA released from dendrites and axon or from axons only is not known. However, as sodium spikes trigger global calcium signals in interneurons, rapid inhibitory interneuron-TC transmission could arise from both axonal and dendritic release sites.

In the presence of TTX, somatic current injections of 100–600 pA for 10–40 ms induced an early passive interneuron depolarization that triggered delayed dendritic calcium spikes (Figure 3D, top in red). Interneuron calcium spikes evoked slow (t_{10-90} > 20 ms) IPSCs in TC cells (Figure 3D, bottom in red), which were also mediated by $GABA_A$ receptor activation (n = 5, data not shown). In trials where depolarizing pulses did not generate presynaptic calcium spikes, postsynaptic IPSCs were greatly reduced in amplitude (Figure 3D, blue), underlining the critical role of calcium spikes in triggering GABA release. As these spikes elevate calcium throughout interneuron dendrites but do not propagate down the axon, slow GABAergic currents likely evoke exclusively global dendritic release.

Calcium spikes could also be evoked by hyperpolarizing current injection in the presence of TTX (Figure S2). Similar rebound calcium spikes have been observed in other types of cells, including the periglomerular cells in the olfactory bulb (Murphy et al., 2005). Calcium spikes evoked in this manner also led to large dendritic calcium signals, did not increase calcium in the axon, and triggered slow GABA release from interneuron dendrites only (Figure S2).

Dendritic L-type calcium channels have been suggested to play a key role in controlling dendritic signaling in other brain regions (Murphy et al., 2005). To determine whether this channel subtype regulates rapid and/or delayed inhibitory interactions between interneurons and TC cells, we examined the effect of nimodipine on sodium- and calcium spike-mediated IPSCs recorded from TC cells (Figures 3E and 3F). Nimodipine had little effect on IPSCs evoked by sodium spikes (Figure 3E, n = 7), but greatly reduced the amplitude of slow IPSCs evoked by

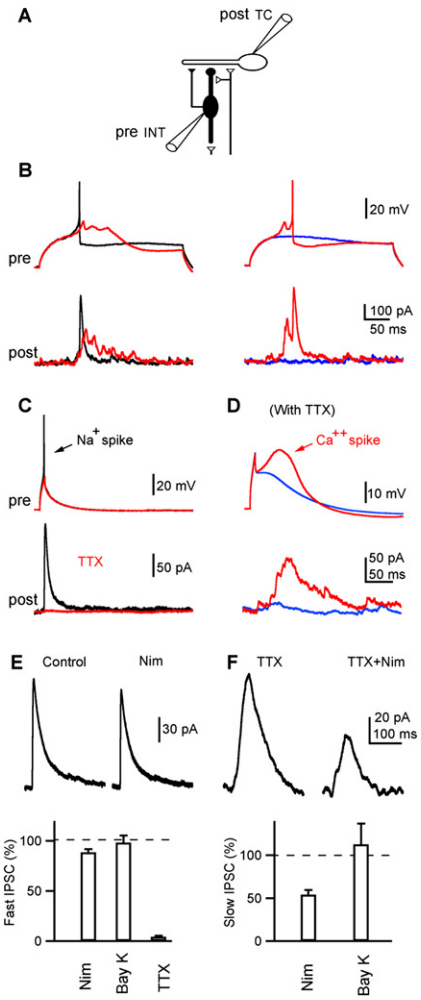

Figure 3. Calcium Spikes Evoke Widespread GABA Release from Interneuron Dendrites

(A) Schematic of experimental configuration.

(B) (Left) Somatic depolarization triggers either a fast (top, back) or a slow (top, red) active response in interneurons, leading to rapid or more prolonged IPSCs, respectively (bottom traces). (Right) Interneuron activation could also evoke a slow active depolarization that led to fast presynaptic action potentials and both slow and rapid postsynaptic currents (red traces). In trials where current injection failed to evoke active interneuron depolarization, no postsynaptic currents were observed (blue traces). (C) Single TTX-sensitive sodium spikes in the interneuron evoked fast GABAergic currents in the TC cell. (D) In TTX, stronger interneuron depolarization triggered regenerative calcium spikes in some trials (single trial, top, red), which evoked slow postsynaptic GABAergic currents (bottom, red). In another trials where depolarization failed to evoke a full-fledged calcium spike (top, blue), there was only a minor deviation from the passive response, and the IPSC was much smaller (bottom, blue). The effects of nimodipine on IPSCs evoked by sodium (E) or calcium (F) spikes are shown for representative experiments (top) and are summarized for seven (E) and six (F) experiments (bottom). Resting membrane potentials were (in mV) −70 for (B), −60 for (C), and −65 for (D).

calcium spikes (Figure 3F, n = 6). Application of the L-type calcium channel activator S-(-)-BayK8644 (Bay K, 10 μM) following nimodipine washout recovered the inhibitory actions of nimodipine on slow IPSCs (Figure 3F, bottom, right), further supporting the idea that this calcium channel subtype is involved in regulating GABA release from dLGN interneuron dendrites.

Thus, active sodium and calcium conductances allow interneurons to release GABA in a widespread manner but with distinct temporal properties. Sodium spikes evoke fast release by rapidly elevating calcium throughout the axons and dendrites. Calcium spikes lead to long-lived calcium transients that trigger slow dendritic release but fail to propagate down the axon. Our results show that activation of dLGN interneurons can lead to widespread GABA release. However, the synaptic mechanisms that evoke these forms of GABA release under more physiological conditions are not known.

Triggering Distinct Interneuron Firing Modes

To provide insight into the manner in which more physiological RGC activation can control GABA release, we determined the strength and number of RGC inputs required to evoke sodium or calcium spikes by stimulating the optic tract at progressively higher intensities (from 0 to 60 μA) while recording from LGN interneurons. Increasing the stimulus intensity resulted in discrete step-like increases in postsynaptic current amplitudes, indicating the sequential recruitment of RGC fibers (Figures 4A and 4B). A similar approach has been used to characterize a number of different types of synapses (Chen and Regehr, 2000; Hooks and Chen, 2006; Lichtman, 1977; Mariani and Changeux, 1981). In 22 of 28 experiments, optic tract stimulation (60 μA) led to convergent activation of three or four RGC inputs onto interneurons (Figure 4D). When tested in current clamp (Figure 4C), coincident activation of several RGC axons could trigger either a burst of sodium spikes riding on a calcium spike (top), a calcium spike alone (middle), or a single sodium spike (bottom). Thus, synchronous activation of multiple convergent RGCs is required to evoke active interneuron firing, but what controls whether LGN interneurons fire a single sodium spike, a calcium spike in isolation, or a calcium spike along with long-latency sodium spikes?

We addressed this question by stimulating the optic tract and measuring interneuron responses in current clamp with cells at progressively more negative membrane potentials (V_m) (Zhu et al., 1999). As shown for a representative experiment (Figure 5), changing the membrane potential switched the firing mode of interneurons in all four cells tested in which synaptic activation could elicit both a calcium spike and a sodium spike. When the optic tract was stimulated at −45 μA to −60 μA, the response mode shifted from a single short-latency sodium spike (Figure 5A, V_m of −60 mV) to a calcium spike sometimes associated with a long-latency sodium spike (Figure 5B, V_m of −70 mV) or to a prolonged calcium spike along with a burst of sodium spikes (Figure 5C, V_m of −75 mV). Thus, large synaptic inputs evoked single short-latency spikes at slightly depolarized potentials, and calcium spikes at more negative potentials. These results suggest that changes in membrane potential allow LGN interneurons to shift their firing mode and thereby alter their spatial and temporal profile of GABA release.

Interneuron Calcium Dynamics Evoked by Synaptic Activation

We then studied the calcium dynamics associated with these distinct synaptically evoked firing patterns. Calcium imaging

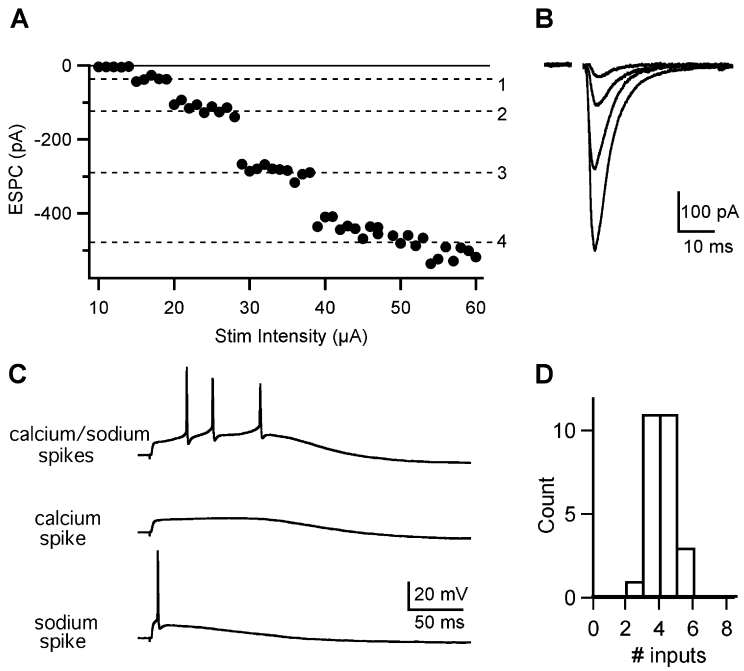

Figure 4. Coincident Activation of Several RGCs Is Required to Trigger Active Interneuron Firing

(A) EPSC amplitudes plotted as a function of the optic tract stimulus intensity in a representative LGN interneuron. (B) Current traces from the same experiment showing the progressive recruitment of RGC inputs with increasing stimulation intensity. (C) Voltage traces from the same experiment showing the different types of active interneuron responses observed when four RGC inputs were synchronously activated (−60 μA stimulation intensity). (D) Histogram showing the number of inputs recruited in individual LGN interneurons when the intensity of the optic tract stimulation was increased from 0 to 60 μA (n = 26). In most cells, 60 μA optic tract stimulation led to convergent activation of three to four inputs to interneurons. $V_{(h)}$ for (B), −60 mV; resting membrane potential for (C), −61 mV.

experiments were performed under similar experimental conditions as described above. As shown in a representative experiment, strong OT stimulation that evoked coincident activation of several RGC axons triggered a burst of sodium/calcium spikes in interneurons (Figure 6B, top in black), leading to large and long-lasting (~500 ms) dendritic calcium increases (Figures 6A and 6B, blue). In contrast, calcium signals measured in axonal boutons were smaller and decayed more rapidly (Figures 6A and 6B, red). In four similar experiments, fluorescent transients were consistently observed throughout the dendrites and axons, but changes in fluorescence were consistently much larger in the dendrites than in the axon (Figure 6C), corresponding to 440 ± 72 nM (n = 17) increases in the dendrites and 94 ± 14 nM (n = 6) increases in axons. These results are consistent with the view that both sodium and calcium spikes account for dendritic calcium elevations, whereas only sodium spikes increase calcium within the axon.

Similar stimulating conditions could also evoke either a calcium spike or a single sodium spike (Figures 4C, 5, and 6D–6F). Synaptically evoked calcium spikes led to slow dendritic calcium elevations throughout the dendrites (Figure 6E, 16 regions in four experiments). The signals peaked ~50 ms after stimulation, consistent with the slow time course of calcium plateau potentials. OT stimulation that triggered sodium spikes in the absence of an obvious calcium plateau potential, as in Figure 6F (top), also triggered widespread calcium signals (31 regions in five experiments). These signals were smaller and much faster (peaked 2–4 ms after stimulation) than those associated with a calcium spike.

Thus, distinct interneuron firing modes dynamically regulate the timing and spatial profile of feedforward inhibition in TC cells. While single sodium spikes account for rapid time-locked inhibition, prolonged calcium spikes and bursts of sodium spikes can lead to delayed disynaptic inhibition due to GABA release from dendrites only or in a widespread manner from dendrites and axon, respectively.

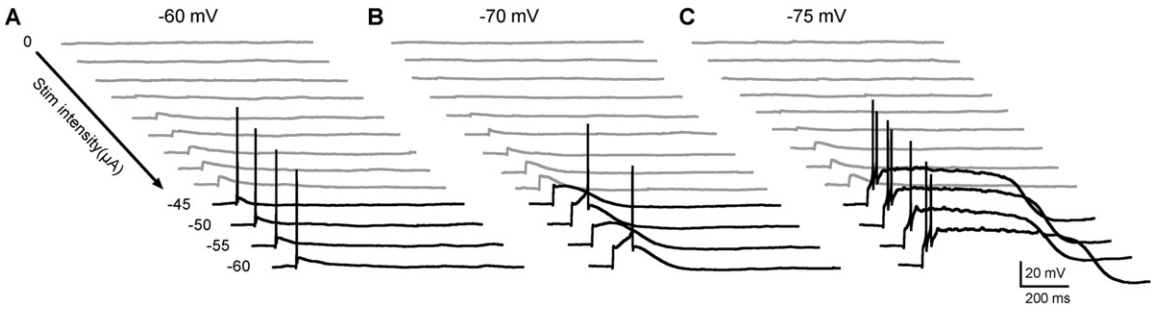

Figure 5. Changes in Membrane Potential Allow Interneurons to Switch between Different Modes of Active Firing

Current-clamp recordings from LGN interneurons were performed while stimulating the optic tract at progressively higher intensities from 0 to −60 μA (indicated by the black arrow in [A], 5 μA steps). In this representative experiment, the same RGC stimulus protocol was repeated when the interneuron was maintained at −60 (A), −70 (B), or −75 mV (C). Strong OT stimulation, which led to active firing (−45 to −60 μA, red), evoked distinctive firing modes in interneurons that were dependent on the initial membrane potential.

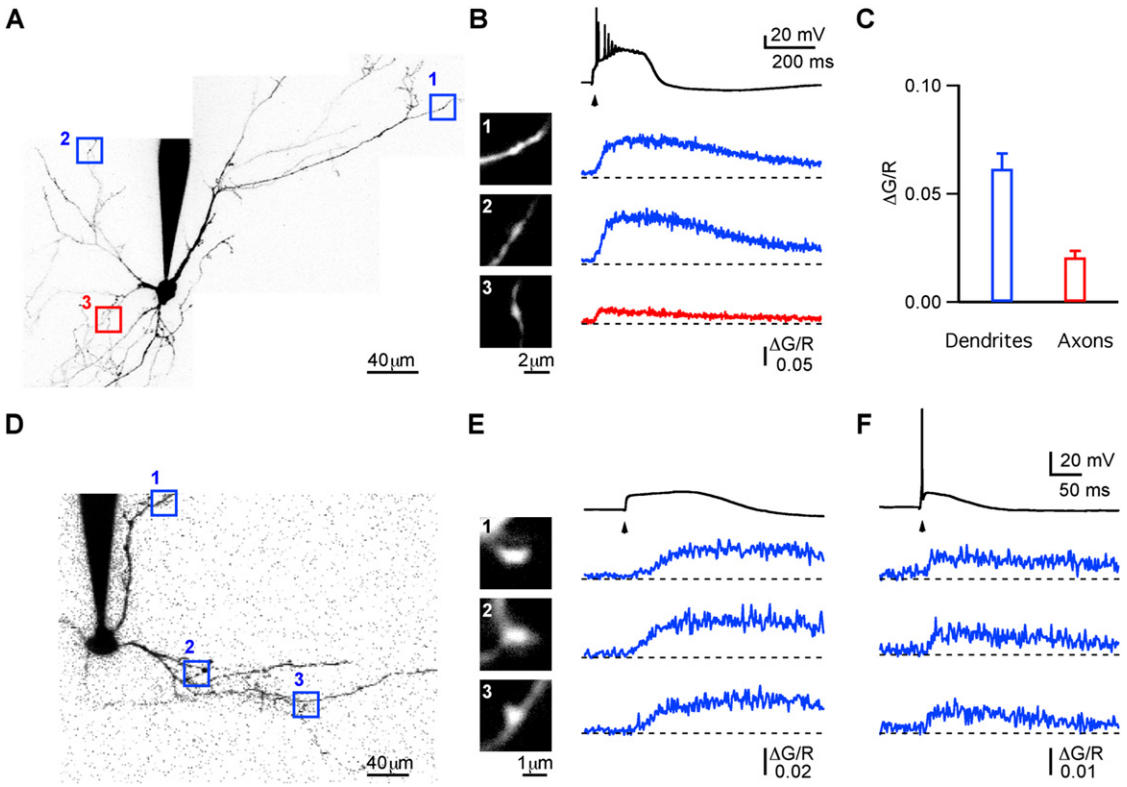

Figure 6. Spatial and Temporal Properties of Dendritic Calcium Dynamics Triggered by Synaptically Evoked Interneuron Firing

Calcium signals are shown that were evoked by coincident activation of several RGC inputs that triggered bursts of calcium/sodium spikes (A–C), individual calcium spikes (D and E), or individual sodium spikes (D and F). (A and D) Inverted fluorescence images of interneurons with dendritic (blue) and axonal (red) regions selected for imaging. (B) OT stimulation triggered a burst of sodium and calcium spikes (top, black trace), leading to prolonged calcium elevation throughout interneuron dendrites (blue) and transient and smaller calcium increases in the axon (red). (C). Summary of the relative amplitude (ΔG/R) of dendritic (blue) and axonal (red) calcium signals triggered by burst interneuron firing following RGC activation (blue, n = 28, red, n = 11). (E and F) Stimulation of several RGC axons in a different interneuron evoked either a calcium spike (E) (top, in black) or a single sodium spike (F) (top, in black) that triggered slow (E) or fast (F) widespread dendritic calcium transients, respectively. Calcium measurements in (E) and (F) were obtained from the same dendritic regions depicted in (D) and (E). Resting membrane potentials were (in mV) −66 for (B) and −62 for (E) and (F).

Properties of Feedforward Inhibition in the LGN

We then studied the properties of feedforward inhibition onto TC cells by stimulating groups of RGC axons, as can occur in response to visual stimulation (Usrey and Reid, 1999), and examining inhibition mediated by activation of local LGN interneurons. Coincident stimulation of multiple RGC fibers evoked a biphasic response in TC neurons that consisted of a monosynaptic EPSC followed by a disynaptic IPSC mediated by local interneurons (Figure 7A, left). EPSCs and IPSCs could be isolated at a holding potential of −60 mV and +7 mV, respectively, and at −10 mV they could be studied simultaneously (Figure 7A, right). Adjusting the position of the stimulus electrode within the optic tract as well as the strength of extracellular stimulation allowed us to identify two forms of inhibition with distinct temporal properties; relatively low intensity optic tract stimulation (20–30 μA) evoked a short-latency EPSC followed by an IPSC with a delay of 1 ms in some neurons (Figure 7B, top left), whereas in others cases long-latency asynchronous (range: 5–150 ms) IPSCs were observed (Figure 7B, top right). Interestingly, higher stimulus intensities (40–60 μA) resulted in a rapid disynaptic IPSC followed by long-latency inhibitory currents in the same cells (Figure 7B, bottom). Together, these results establish that distinct modes of feedforward inhibition exist within the LGN, which can be sequentially recruited by increasing the number of synchronously activated RGCs.

AMPA receptors and NMDA receptors, which have rapid and slow kinetics, respectively, are both present on interneuron dendrites (Pape and McCormick, 1995), but their relative contributions to rapid and delayed forms of disynaptic inhibition have not been determined. We therefore assessed the effects of ionotropic glutamate receptor antagonists on short- or long-latency inhibitory current recorded in TC cells while performing strong extracellular stimulation of the optic tract. Blockade of NMDA receptors in interneurons reduced fast IPSCs by 41% ± 9% and delayed inhibition by 62% ± 6% (Figures 7C and 7D). Subsequent addition of the AMPA receptor antagonist NBQX (10 μM) completely eliminated the remaining inhibitory disynaptic currents (Figures 7C and 7D), further supporting the critical role played by ionotropic glutamate receptors in triggering GABA release from LGN interneurons.

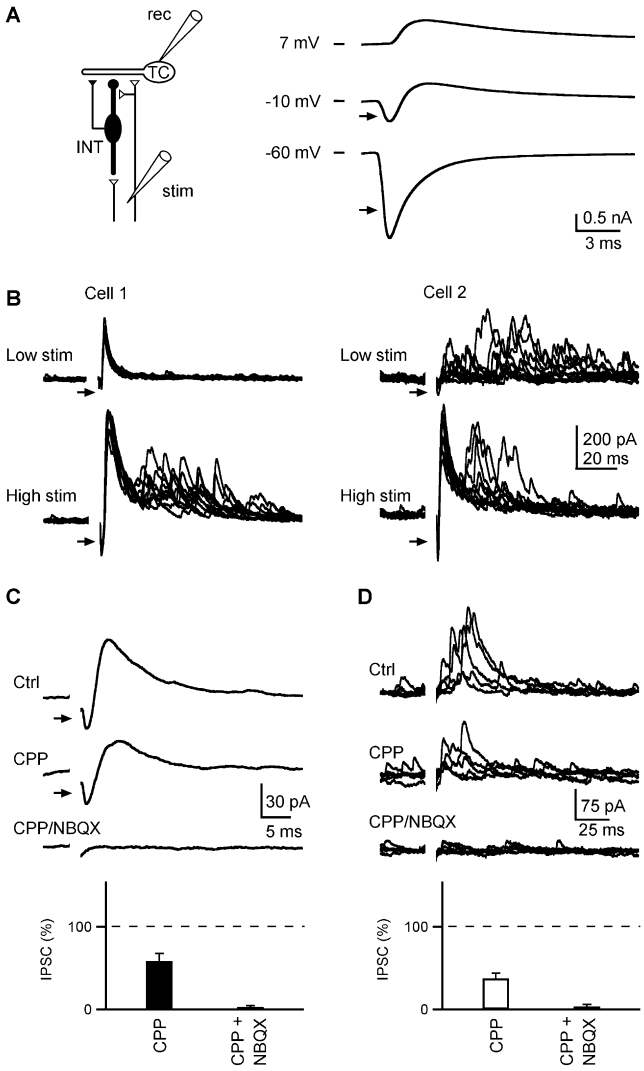

Figure 7. Temporal Properties of Feedforward Inhibition within the LGN

(A) (Left) Diagram of recording configuration. (Right) Monosynaptic EPSCs (inward) and disynaptic IPSCs (outward) recorded at three different holding potentials. Black arrows indicate monosynaptic excitation of TC cells in (A)–(C). (B) (Top) Low-intensity OT stimulation evoked fast inhibition in cell 1 and delayed inhibition in cell 2. (Bottom) High-intensity OT stimulation evoked both forms of inhibition in these cells. Effects of NMDA receptor antagonist (CPP) and NMDA/AMPA receptor blockade (CPP + NBQX) on rapid (C) and delayed (D) feedforward IPSCs are shown for representative experiments (top, [C and D]) and are summarized for 27 (bottom left) and 10 (bottom right) experiments, respectively. $V_{(h)}$, −10 mV for all experiments.

Contribution of L-Type Calcium Channels to Disynaptic Inhibition in the LGN

We have shown that calcium spikes mediated by activation of L-type calcium channels in interneurons trigger dendritic GABA release. To determine the mechanisms by which L-type calcium channels modulate feedforward inhibition under more physiological conditions, we recorded either from LGN interneurons or from TC cells while stimulating convergent RGC axons. These experiments were performed in the presence of the NMDAR antagonist CPP to isolate the role of L-type calcium channels. When interneurons were voltage clamped and RGCs were activated, RGC→interneuron EPSCs were unaffected by nimodipine (Figure S3, n = 8), indicating that nimodipine does not act presynaptically on RCG axons. In contrast, responses measured in current clamp were highly sensitive to nimodipine. When recording from interneurons in current clamp, the stimulation intensity was adjusted so that it was just above the threshold required to trigger active responses that consisted of a single sodium spike, a single calcium spike, or a calcium spike and a burst of sodium spikes (Figures 8A and 8B). The blockade of L-type calcium channels with nimodipine prevented the firing of synaptically evoked single sodium spikes (Figure 8A). In another experiment, synaptic activation resulted in a slow calcium plateau (Figure 8B, top in red) or a calcium plateau and burst of sodium spikes (Figure 8B, top in black). Nimodipine also abolished synaptically evoked calcium spikes and thereby prevented the generation of late sodium spikes (Figure 8b, middle trace). Application of BayK following nimodipine washout recovered active interneuron responses (Figure 8B, lower traces).

These results suggest that L-type calcium channels in interneurons could regulate disynaptic inhibition through several mechanisms. L-type calcium channels could regulate the rapid release of GABA, by regulating the likelihood of synaptically evoking a sodium spike in interneurons (even though L-type calcium channels do not regulate IPSCs following sodium spikes initiated by somatic current injection, Figure 3E) or by contributing to dendritic calcium transients evoked by individual sodium spikes (Figure S4). L-type calcium channels could also regulate delayed IPSCs in TC cells by controlling GABA release from interneurons triggered by slow calcium spikes in the dendrites and/or long-latency sodium spikes in dendrites and axons (Figures 3D and 8B).

To understand how L-type calcium channel actions on interneuron firing might affect GABA release, we assessed the effect of nimodipine and BayK on synaptically evoked short- and long-latency inhibition recorded in TC neurons. As shown in an experiment in which an RGC→TC EPSC and a rapid disynaptic IPSC were monitored (Figure 8C), nimodipine reduced rapid disynaptic inhibition by ~40% but did not affect the EPSC (black arrows). In another experiment in which delayed disynaptic IPSCs were observed in isolation, nimodipine almost eliminated delayed IPSCs (Figures 8D and 8E). Overall, nimodipine reduced the rapid component of the IPSC by 38% ± 5% (n = 27) and the delayed component by 82% ± 6% (n = 10). Nifedipine (10 μM), another blocker of L-type calcium channels, had similar effects, reducing fast IPSCs by 44% and slow IPSCs by 87% (n = 8). In general, the washouts of nimodipine and nifedipine were incomplete. However, the subsequent bath application of S-(-)-BayK8644 during the washout of nimodipine enhanced the actions of the L-type blockers on feedforward inhibition in TC cells (Figures 8E and 8F).

We also evaluated the contribution of L-type calcium channels to feedforward inhibition when dendritic NMDA receptors were intact in LGN interneurons. Under these conditions, we found that nimodipine reduced rapid IPSCs by 46% ± 6% and delayed inhibition by 48% ± 11% (Figure 8F and Figure S5). Thus, L-type calcium channels contribute to rapid and delayed inhibition in the

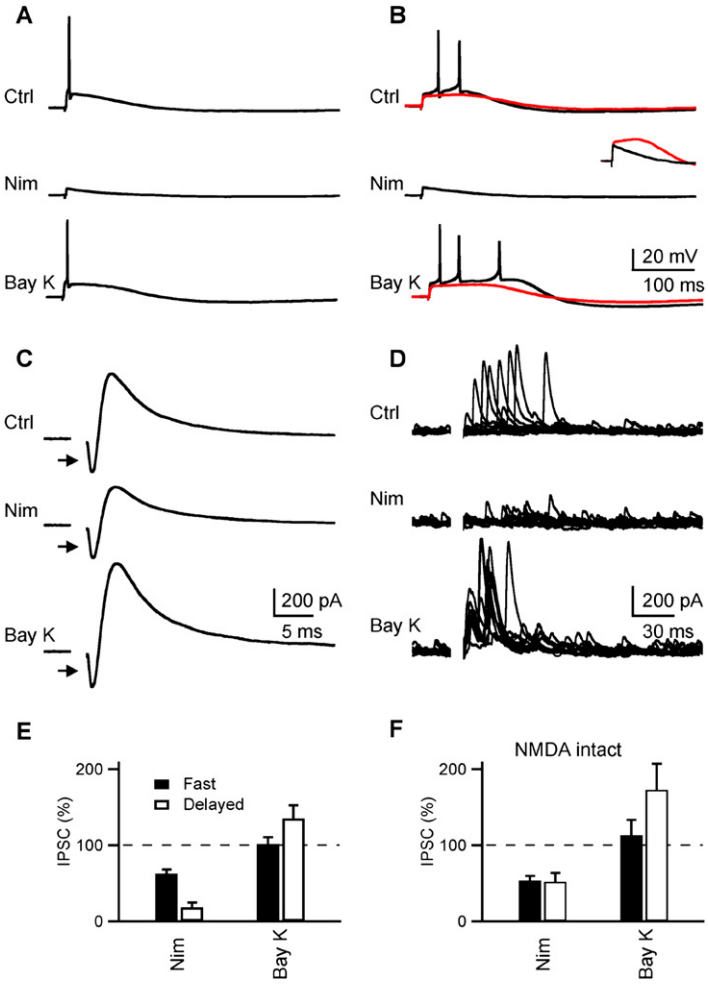

Figure 8. Dendritic L-Type Calcium Channels Regulate Interneuron Firing and Both Fast and Delayed Disynaptic Inhibition in TC Cells

(A and B) Effects of nimodipine and BayK on interneuron firing (single sodium spikes in [A], single calcium spike in [B] [red], or burst of calcium/sodium spikes in [B] [black]) triggered by strong stimulation of the optic tract. Insert in (B) shows nimodipine effects on calcium spike (red trace from [B], upper and black trace from [B], middle). Scale for insert: 8 mV and 125 ms. (C–E) L-type calcium channel regulation of disynaptic inhibition in TC cells. Effects of nimodipine and BayK on fast (C) and delayed (D) feedforward IPSCs are shown for representative experiments and are summarized (E) (left) for 27 (filled bars) and 10 (open bars) experiments, respectively. (F) Summery graph showing the contribution of L-type calcium channels to feedforward IPSCs with interneuron NMDA receptors intact (n = 7 and n = 6 for fast and delayed IPSCs, respectively). $V_{(h)}$, −10 mV for all experiments.

absence of NMDA receptor blockade. These results illustrate that dendritic L-type calcium channels in interneurons can regulate GABAergic transmission on both rapid and slow timescales.

DISCUSSION

We found that active conductances of LGN interneurons play an important role in regulating feedforward inhibition to TC neurons. Synchronous activation of subsets of RGCs triggers action potentials in interneurons. Sodium action potentials evoke widespread calcium signals throughout dendritic and axonal arbors, whereas calcium spikes mediated by L-type calcium channels trigger dendritic GABA release. Sodium and calcium spikes regulate the rapid and prolonged release of GABA from interneurons that gives rise to the disynaptic inhibitory responses in TC cells. Thus, active dendritic conductances in interneurons dynamically regulate the spatial and temporal features of feedforward inhibition within the LGN.

Sodium and Calcium Action Potentials in LGN-Interneuron Dendrites

An important property of LGN interneurons is that they can release GABA from their dendrites (Cox and Sherman, 2000; Cox et al., 1998; Famiglietti and Peters, 1972; Hamos et al., 1985; Rafols and Valverde, 1973), but whether the dendrites support action potentials and whether active dendritic conductances affect dendritic signaling was not known (Sherman, 2004). We found that sodium spikes triggered rapid elevations of calcium throughout the dendrites and axons of interneurons. Several lines of evidence suggest that this widespread profile of dendritic calcium elevations likely reflects active propagation of sodium spikes. First, the blockade of voltage-dependent sodium channels with TTX eliminates rapid dendritic calcium signals. Second, using somatic depolarization that leads to generation of sodium action potentials in around 50% of the trials, we find that dendritic calcium accumulation are always associated with all-or-none sodium spikes and never with passive responses. Finally, there was no significant attenuation of the calcium signals for distances of up to 300 μm from the soma. As the dendrites of LGN interneurons are fine (Rafols and Valverde, 1973) and are predicted to have a short space constant (Bloomfield and Sherman, 1989), the lack of attenuation is inconsistent with passive propagation. Thus, widespread propagation of sodium spikes can affect dendritic signaling in interneurons.

The dendrites of LGN interneurons also support calcium spikes that have a number of interesting properties. First, calcium spikes can be triggered by large somatic depolarization, but are much more readily evoked by synaptic inputs. This suggests a dendritic site of origin. Second, calcium spikes trigger large increases in calcium that are restricted to the dendrites. Although in some instances they also trigger a burst of sodium spikes, in other cases calcium spikes are observed in isolation. Thus, calcium spikes are good candidates to selectively affect dendritic signaling in interneurons. Third, calcium spikes and their associated calcium signals last for hundreds of milliseconds, which is much longer than the calcium elevations associated with a sodium action potential. Fourth, calcium spikes are mediated by activation of dendritic nimodipine-sensitive L-type calcium channels. Thus, dendritic L-type calcium channels and dendritic calcium spikes play an important role in calcium signaling in the dendrites of LGN interneurons.

These findings establish that LGN interneurons support both sodium and calcium action potentials. In other types of neurons, considerable diversity has been observed in the ability of dendrites to support action potentials (Goldberg and Yuste, 2005; Waters et al., 2005). Backpropagation of somatically generated sodium spikes is reliable in some types of neurons, whereas in others it is partial or does not occur (Christie and Westbrook, 2003; Egger et al., 2003; Goldberg et al., 2003a, 2003b; Margrie et al., 2001; Martina et al., 2000; Xiong and Chen, 2002; Zelles et al., 2006), often because dendritic A-type potassium channels limit the extent of backpropagation (Christie and Westbrook, 2003; Goldberg et al., 2003b; Hoffman et al., 1997). The lack of attenuation of calcium signals with distance from the soma observed in our experiments suggests that no such mechanism is present in LGN interneurons. The ability of various types of neurons to support calcium spikes, the type of calcium channel mediating the spikes and the extent of spread of calcium spikes are highly variable (Egger et al., 2005; Goldberg et al., 2004; Goldberg and Yuste, 2005; Golding et al., 2002; Kampa and Stuart, 2006; Llinas and Sugimori, 1980; Murphy et al., 2005; Schiller et al., 2000; Wei et al., 2001). The properties of calcium spikes in LGN interneurons are more similar to olfactory periglomerular neurons in that a low-threshold calcium spike mediated by L-type calcium channels produces widespread calcium signals (Murphy et al., 2005). As periglomerular neurons also release neurotransmitter from its dendrites, this suggests that low-threshold calcium spikes may provide a common mechanism to regulate the release of neurotransmitter from dendrites.

Rapid and Delayed Inhibition Provided by LGN Interneurons

The synchronous activation of multiple RGC axons evokes disynaptic inhibition in TC cells that is comprised of a rapid IPSC that follows direct excitation with a delay of just 1 ms, and a late component of inhibition that persists for tens of milliseconds (Figure 6). Inhibition in TC neurons is eliminated by blocking AMPA and NMDA receptors. This indicates that it is disynaptic in nature, requires activation of interneurons through ionotropic glutamate receptors, and that group I metabotropic glutamate receptors (Cox and Sherman, 2000; Godwin et al., 1996; Govindaiah and Cox, 2004) are not involved under our experimental conditions. L-type calcium channels and NMDA receptors within the dendrites of LGN interneurons play an important role in regulating both rapid and delayed inhibition, whereas the contribution of dendritic sodium channels remains unclear.

The observation that sodium spikes evoke widespread calcium signals throughout the cell suggests that they could trigger rapid GABA release from dendrites and axon. Paired recordings established that sodium spikes in interneurons give rise to short-latency inhibition in TC neurons. However, release under such conditions could be mediated by dendrites and/or axons. Although it seems likely that sodium spikes could trigger release from both axons and dendrites, it must be noted that the residual calcium we measured is unlikely to directly trigger neurotransmitter release (Augustine and Neher, 1992; Schneggenburger and Neher, 2005; Zucker and Regehr, 2002). Instead, release is usually driven by local calcium signals that depend upon the proximity of calcium-permeable channels to release sites. As sodium action potentials could trigger very different local calcium signals in axons and dendrites, and the calcium-sensitivity of the release machinery could be different in these compartments, whether sodium action potentials trigger release from the dendrites of LGN interneurons remains an open question.

Remarkably, blocking L-type calcium channels resulted in a near 40% reduction in rapid inhibition. The calcium channels that regulate disynaptic inhibition must be present in the dendrites of LGN interneurons, because L-type calcium channels do not regulate release from RGC boutons. RGC activation must rapidly open dendritic L-type calcium channels to regulate GABA release on such a rapid timescale (Xu and Lipscombe, 2001). L-type calcium channels are unlikely to contribute to rapid disynaptic inhibition by direct actions on the interneuron-TC synapse, because paired recordings show that sodium action potentials trigger rapid inhibitory currents in postsynaptic TC neurons that are insensitive to nimodipine. Instead, it seems more likely that L-type calcium channels could control rapid feedforward inhibition by regulating interneuron sodium spike initiation threshold.

The blockade of L-type calcium channels also reduces delayed inhibition. Recording from interneurons while stimulating multiple RGC axons shows that these cells can fire calcium spikes alone or in conjunction with burst of delayed sodium spikes (Figure 7B). It is likely that L-type calcium channels regulate delayed inhibition in part by generating calcium spikes that evoke dendritic GABA release, as observed for paired recordings between interneurons and TC neurons. In addition, L-type calcium channels can trigger delayed sodium spikes that regulate long-latency release of GABA from axons and possibly dendrites.

The effect of NMDA receptor blockade on disynaptic inhibition in TC neurons establishes that these receptors contribute to both rapid and delayed inhibition. The contribution of NMDARs to short-latency inhibition is somewhat surprising, because these receptors have slower kinetics than AMPA receptors. Clearly, however, RGC activation must open them in less than a millisecond. Blockade of both NMDA receptors and L-type calcium channels is required to eliminate delayed inhibition, indicating that these channels work together to trigger delayed transmitter release. NMDARs or L-type calcium channels could evoke release directly by admitting calcium (MacDermott et al., 1986), or indirectly by providing long-lasting depolarization to allow calcium influx through other calcium-permeable channels (Murphy et al., 2005; Schiller et al., 2000). The ability of NMDA receptors and L-type calcium channels to regulate disynaptic inhibition is not universally observed throughout the brain. However, NMDARs and L-type calcium channels also regulate neurotransmitter release from the dendrites of periglomerular cells in the olfactory bulb (Murphy et al., 2005), suggesting that dendritic release in the visual and olfactory systems share some common properties.

The number of activated inputs and the initial membrane potential control the firing mode of LGN interneurons. It is necessary to synchronously activate several RGC inputs in order to trigger an active response. The nature of the active response is highly sensitive to membrane potential. A slightly depolarized cell tends to fire single short-latency spikes, whereas a more hyperpolarized cell fires calcium spikes that are often associated

with long-latency sodium spikes. Inhibitory inputs from the reticular nucleus and cholinergic inputs have been shown to hyperpolarize LGN interneurons and shift the membrane potential over a range associated with different firing modes (Cucchiaro et al., 1991, 1993; McCormick and Pape, 1988; McCormick and Prince, 1986; Sherman, 2004).

Conclusion

This study adds to the growing evidence supporting the importance of feedforward inhibition throughout the brain (Callaway, 2004; Carter and Regehr, 2002; Gabernet et al., 2005; Murphy et al., 2005; Pouille and Scanziani, 2001; Pouille and Scanziani, 2004), while highlighting the degree to which interneurons can be specialized. We find that, within the dLGN, interneurons are particularly flexible circuit elements that regulate TC neurons by releasing GABA with distinct spatial and temporal properties. These modes of transmitter release can be dynamically regulated by synchronous firing of subsets of RGCs during visual stimulation. This dynamic form of feedforward inhibition results from the interaction between visually evoked activation of RGCs with intrinsic interneuron properties. We suggest that coincident firing of functionally related RGCs observed in vivo (Usrey and Reid, 1999) plays an important role in shaping the temporal and spatial extent of feedforward inhibition within the LGN and thereby in controlling spike timing and in refining receptive fields in TC neurons.

EXPERIMENTAL PROCEDURES

Animals

LGN GABAergic interneurons were identified by using C57BL/J6 GAD67-GFP (neo) transgenic mice (kindly provided by Yuchio Yanagawa) that selectively expressed GFP under the control of the endogenous *GAD67* gene promoter as described previously (Marowsky et al., 2005; Tamamaki et al., 2003). In most of the experiments in which TC cell activity was monitored, slices were prepared from normal wild-type C57BL/J6 mice.

Slice Preparation and Electrophysiology

Mice (C57BL/J6, 23–32 days old) were deeply anesthetized with nembutal, and their brains were rapidly removed and placed in ice-cold oxygenated (95% O_2, 5% CO_2) high-sucrose solution that contained (in mM) 220 sucrose, 2.5 KCl, 6 $MgCl_2$, 1 $CaCl_2$, 1.25 NaH_2PO_4, 26 $NaHCO_3$, 10 glucose. A block of tissue containing the thalamus was excised and transferred to a vibratome, where 200–250 μm pseudosagittal slices were obtained as described previously (Blitz and Regehr, 2005; Chen and Regehr, 2000). Then, slices containing the LGN and intact optic tract were gently moved to an equilibrium chamber filled with oxygenated artificial CSF (ACSF) that contained (in mM) 124 NaCl, 3 KCl, 2 $MgCl_2$, 2 $CaCl_2$, 1.23 NaH_2PO_4, 26 $NaHCO_3$, 10 glucose. After 1–2 hr of recovery from sectioning, the slices were transferred to a recording chamber mounted on an Olympus BX51WI upright microscope. Tissue was continuously superfused with ACSF at ~5 ml/min flow rate. The microscope was equipped with video-enhanced infrared-differential interference contrast (DIC) and fluorescence capabilities. The temperature in the recording chamber was kept near 34°C using an inline heater controller (Warner Instruments, Hamden, CT).

Whole-cell voltage- and current-clamp recordings from LGN interneurons were performed by using 2.5–3.5 MΩ borosilicate glass pipettes filled with an intracellular solution that contained the following (in mM): 150 $CsMeSO_4$ (or $KMeSO_4$ for current-clamp recordings), 1 $MgCl_2$, 10 HEPES, 0.5 EGTA, 2 Mg-ATP, 0.4 Na_2-GTP, and 10 Na_2-phosphocreatine, pH 7.3 with CsOH (or KOH for $KMeSO_4$-based solution). In the experiments in which paired recordings from interneurons and TC cells were performed, a gluconate-based pipette solution was used and contained (in mM) 150 KGluconate, 1 $MgCl_2$, 5 HEPES, 1.1 EGTA, 2 Mg-ATP, 10 Na_2-phosphocreatine, pH 7.3 with KOH. In some paired recording experiments, stimulation of LGN interneurons was performed in cell-attached configuration to prevent presynaptic rundown of transmitter release. GABAergic GFP-expressing LGN interneurons were identified under fluorescence, and then DIC was used to approach the cells and achieve gigaseal configuration. In all LGN interneuron recordings, both $GABA_A$ and $GABA_B$ receptor subtypes were blocked by bath application of 10 μM picrotoxin and 2 μM CGP55845, respectively.

Voltage-clamp recordings from TC cells were made with 1.8–2.4 MΩ borosilicate glass pipettes filled with an internal solution containing (in mM) 130 CsGluconate, 10 $CsCl_2$, 2 $MgCl_2$, 10 HEPES, 0.16 $CaCl_2$, 0.5 EGTA, 4 Na_2-ATP, 0.4 Na_2-GTP, 14 Tris-creatine phosphate, 20 TEA-acetate adjusted to pH 7.3 with CsOH. Whole-cell mode was obtained after gentle application of negative pressure through the recording pipette by using a glass syringe. Slow and fast capacitive components were automatically compensated. Access resistance was monitored throughout the experiments, and only those cells with stable access resistance (changes <10%) were used for analysis. The recordings were performed with a MultiClamp 700B amplifier (Axon Instruments) and were controlled with custom software written in Igor Pro (WaveMetrics, Lake Oswego, OR) kindly provided by Matthew Xu-Friedman. RGC axons were stimulated extracellularly using a theta glass electrode filled with ACSF and placed in the optic tract around 1 mm away from recorded cells. Brief (300 μs, 0–60 μA) electrical pulses were delivered (every 10–30 s) through an A395 Linear Stimulus Isolator (WPI). All recording were performed in the presence of 2 μM CGP55845 to block $GABA_B$ receptors. In some recording from TC neurons, 5 μM CPP was added to the bath to block NMDA receptors in both TC cells and interneurons (i.e., Figure 6). The remaining TC experiments were done with 1–2 mM MK801 in the recording pipette to block NMDA receptors in postsynaptic TC cells but not in LGN interneuron dendrites. Peak amplitude and integrated charge (5–150 ms) were computed for analysis of fast and delayed inhibitory currents, respectively.

Calcium Imaging

Two-photon calcium-imaging experiments were performed using a custom two-photon laser scanning microscope with a 60×, 1.1 NA objective and a titanium/sapphire laser (Mira; Coherent, Santa Clara, CA) tuned to 810 nm for excitation, and controlled with custom software written in Matlab (MathWorks, Natick, MA), kindly provided by Bernardo L Sabatini. LGN interneurons were loaded with the calcium indicator fluo-5F (100 μM) and the fluorescent dye Alexa 594 (50 μM) for visualization of interneuron processes. Green and red fluorescence were separated using a 565 nm dichroic and filtered using 555 nm short-pass filter and a 607/45 band-pass filter, respectively, and collected using R3896 R9110 and H7422 photomultiplier tubes (Hamamatsu, Hamamatsu City, Japan). Calcium measurements were made in line-scan mode at 0.5 KHz in dendritic protrusions or in bouton-like structures along dendrites and axons. Regions of interest were scanned for 0.25–0.5 s for sodium spike-evoked transients and for 0.5–2.5 s for transients due to calcium spikes. Both sodium and calcium spikes were evoked by either somatic current injection or by synaptic activation of multiple RGC axons. Fluorescence signals were converted to calcium concentration in a subset of experiments by using values of R_{min} and R_{max} measured in the same imaging system with internal solutions containing 0 mM Ca^{2+}/5 mM EGTA and 5 mM Ca^{2+}, respectively. The K_D for Fluo 5F under similar experimental conditions has been previously reported to be ~600 μM.

In a subset of experiments (contribution of L-type channels to calcium transients evoked by calcium spikes), calcium imaging was done with a Cooke (Romulus, MI) Sensicam QE CCD camera mounted on an Olympus (Tokyo, Japan) BX51WI upright microscope equipped with a 60×, 0.9 NA objective. In these experiments, interneurons were loaded with the calcium indicator fura-2 (100 μM) through the recording pipette. Fura-2 was excited at 380 nm with a monochromator (Polychrome IV; TILL Photonics, Gräfelfing, Germany). The filter set used included a 415 nm dichroic (TILL Photonics) and 515LP for emission (Omega Optical, Brattleboro, VT). Images were acquired with 20 ms exposures at 20 Hz. For all imaging experiments, calcium indicators were dissolved in a current-clamp internal solution containing (in mM) 150 $KMeSO_4$, 1 $MgCl_2$, 10 HEPES, 2 Mg-ATP, 0.4 Na_2-GTP, and 10 Na_2-phosphocreatine, pH 7.3 with KOH.

Data Analysis and Statistics

Igor Pro software was used for analysis. Data in Results are expressed as mean ± SEM. Statistical analyses were performed using one-way ANOVA followed by a Bonferroni post hoc procedure for pairwise between-group comparison (i.e., control, treatment 1, treatment 2). The nonparametric Kolmogorov-Smirnov test was used for comparison of the cumulative fractions. A value of $p < 0.05$ was considered statistically significant.

Supplemental Data

The Supplemental Data for this article can be found online at http://www.neuron.org/cgi/content/full/57/3/420/DC1/.

ACKNOWLEDGMENTS

We thank John Assad and members of the Regehr laboratory for their critical comments on this manuscript and Dawn Blitz for guidance in the initial phase of this project. This work was supported by NIH grant R37-NS322405 and Dana/Mahoney Fellowship Fund.

Received: August 27, 2007
Revised: November 14, 2007
Accepted: December 17, 2007
Published: February 6, 2008

REFERENCES

Augustine, G.J., and Neher, E. (1992). Neuronal Ca2+ signalling takes the local route. Curr. Opin. Neurobiol. *2*, 302–307.

Berardi, N., and Morrone, M.C. (1984). The role of gamma-aminobutyric acid mediated inhibition in the response properties of cat lateral geniculate nucleus neurones. J. Physiol. *357*, 505–523.

Blitz, D.M., and Regehr, W.G. (2005). Timing and specificity of feed-forward inhibition within the LGN. Neuron *45*, 917–928.

Bloomfield, S.A., and Sherman, S.M. (1989). Dendritic current flow in relay cells and interneurons of the cat's lateral geniculate nucleus. Proc. Natl. Acad. Sci. USA *86*, 3911–3914.

Brenowitz, S.D., Best, A.R., and Regehr, W.G. (2006). Sustained elevation of dendritic calcium evokes widespread endocannabinoid release and suppression of synapses onto cerebellar Purkinje cells. J. Neurosci. *26*, 6841–6850.

Callaway, E.M. (2004). Feedforward, feedback and inhibitory connections in primate visual cortex. Neural Netw. *17*, 625–632.

Carter, A.G., and Regehr, W.G. (2002). Quantal events shape cerebellar interneuron firing. Nat. Neurosci. *5*, 1309–1318.

Chen, C., and Regehr, W.G. (2000). Developmental remodeling of the retinogeniculate synapse. Neuron *28*, 955–966.

Christie, J.M., and Westbrook, G.L. (2003). Regulation of backpropagating action potentials in mitral cell lateral dendrites by A-type potassium currents. J. Neurophysiol. *89*, 2466–2472.

Cox, C.L., and Sherman, S.M. (2000). Control of dendritic outputs of inhibitory interneurons in the lateral geniculate nucleus. Neuron *27*, 597–610.

Cox, C.L., Zhou, Q., and Sherman, S.M. (1998). Glutamate locally activates dendritic outputs of thalamic interneurons. Nature *394*, 478–482.

Cruikshank, S.J., Lewis, T.J., and Connors, B.W. (2007). Synaptic basis for intense thalamocortical activation of feedforward inhibitory cells in neocortex. Nat. Neurosci. *10*, 462–468.

Crunelli, V., Haby, M., Jassik-Gerschenfeld, D., Leresche, N., and Pirchio, M. (1988). Cl- - and K+-dependent inhibitory postsynaptic potentials evoked by interneurones of the rat lateral geniculate nucleus. J. Physiol. *399*, 153–176.

Cucchiaro, J.B., Uhlrich, D.J., and Sherman, S.M. (1991). Electron-microscopic analysis of synaptic input from the perigeniculate nucleus to the A-laminae of the lateral geniculate nucleus in cats. J. Comp. Neurol. *310*, 316–336.

Cucchiaro, J.B., Uhlrich, D.J., and Sherman, S.M. (1993). Ultrastructure of synapses from the pretectum in the A-laminae of the cat's lateral geniculate nucleus. J. Comp. Neurol. *334*, 618–630.

Denk, W., Strickler, J.H., and Webb, W.W. (1990). Two-photon laser scanning fluorescence microscopy. Science *248*, 73–76.

Egger, V., Svoboda, K., and Mainen, Z.F. (2003). Mechanisms of lateral inhibition in the olfactory bulb: efficiency and modulation of spike-evoked calcium influx into granule cells. J. Neurosci. *23*, 7551–7558.

Egger, V., Svoboda, K., and Mainen, Z.F. (2005). Dendrodendritic synaptic signals in olfactory bulb granule cells: local spine boost and global low-threshold spike. J. Neurosci. *25*, 3521–3530.

Famiglietti, E.V., Jr. (1970). Dendro-dendritic synapses in the lateral geniculate nucleus of the cat. Brain Res. *20*, 181–191.

Famiglietti, E.V., Jr., and Peters, A. (1972). The synaptic glomerulus and the intrinsic neuron in the dorsal lateral geniculate nucleus of the cat. J. Comp. Neurol. *144*, 285–334.

Gabernet, L., Jadhav, S.P., Feldman, D.E., Carandini, M., and Scanziani, M. (2005). Somatosensory integration controlled by dynamic thalamocortical feed-forward inhibition. Neuron *48*, 315–327.

Godwin, D.W., Van Horn, S.C., Eriir, A., Sesma, M., Romano, C., and Sherman, S.M. (1996). Ultrastructural localization suggests that retinal and cortical inputs access different metabotropic glutamate receptors in the lateral geniculate nucleus. J. Neurosci. *16*, 8181–8192.

Goldberg, J.H., and Yuste, R. (2005). Space matters: local and global dendritic Ca2+ compartmentalization in cortical interneurons. Trends Neurosci. *28*, 158–167.

Goldberg, J.H., Tamas, G., Aronov, D., and Yuste, R. (2003a). Calcium microdomains in aspiny dendrites. Neuron *40*, 807–821.

Goldberg, J.H., Tamas, G., and Yuste, R. (2003b). Ca2+ imaging of mouse neocortical interneurone dendrites: Ia-type K+ channels control action potential backpropagation. J. Physiol. *551*, 49–65.

Goldberg, J.H., Lacefield, C.O., and Yuste, R. (2004). Global dendritic calcium spikes in mouse layer 5 low threshold spiking interneurones: implications for control of pyramidal cell bursting. J. Physiol. *558*, 465–478.

Golding, N.L., Staff, N.P., and Spruston, N. (2002). Dendritic spikes as a mechanism for cooperative long-term potentiation. Nature *418*, 326–331.

Govindaiah, and Cox, C.L. (2004). Synaptic activation of metabotropic glutamate receptors regulates dendritic outputs of thalamic interneurons. Neuron *41*, 611–623.

Guillery, R.W., and Sherman, S.M. (2002). Thalamic relay functions and their role in corticocortical communication: generalizations from the visual system. Neuron *33*, 163–175.

Hamos, J.E., Van Horn, S.C., Raczkowski, D., Uhlrich, D.J., and Sherman, S.M. (1985). Synaptic connectivity of a local circuit neurone in lateral geniculate nucleus of the cat. Nature *317*, 618–621.

Hoffman, D.A., Magee, J.C., Colbert, C.M., and Johnston, D. (1997). K+ channel regulation of signal propagation in dendrites of hippocampal pyramidal neurons. Nature *387*, 869–875.

Hooks, B.M., and Chen, C. (2006). Distinct roles for spontaneous and visual activity in remodeling of the retinogeniculate synapse. Neuron *52*, 281–291.

Hubel, D.H., and Wiesel, T.N. (1979). Brain mechanisms of vision. Sci. Am. *241*, 150–162.

Kampa, B.M., and Stuart, G.J. (2006). Calcium spikes in basal dendrites of layer 5 pyramidal neurons during action potential bursts. J. Neurosci. *26*, 7424–7432.

Lichtman, J.W. (1977). The reorganization of synaptic connexions in the rat submandibular ganglion during post-natal development. J. Physiol. *273*, 155–177.

Llinas, R., and Sugimori, M. (1980). Electrophysiological properties of in vitro Purkinje cell dendrites in mammalian cerebellar slices. J. Physiol. *305*, 197–213.

MacDermott, A.B., Mayer, M.L., Westbrook, G.L., Smith, S.J., and Barker, J.L. (1986). NMDA-receptor activation increases cytoplasmic calcium concentration in cultured spinal cord neurones. Nature *321*, 519–522.

Margrie, T.W., Sakmann, B., and Urban, N.N. (2001). Action potential propagation in mitral cell lateral dendrites is decremental and controls recurrent and lateral inhibition in the mammalian olfactory bulb. Proc. Natl. Acad. Sci. USA *98*, 319–324.

Mariani, J., and Changeux, J.P. (1981). Ontogenesis of olivocerebellar relationships. I. Studies by intracellular recordings of the multiple innervation of Purkinje cells by climbing fibers in the developing rat cerebellum. J. Neurosci. *1*, 696–702.

Marowsky, A., Yanagawa, Y., Obata, K., and Vogt, K.E. (2005). A specialized subclass of interneurons mediates dopaminergic facilitation of amygdala function. Neuron *48*, 1025–1037.

Martina, M., Vida, I., and Jonas, P. (2000). Distal initiation and active propagation of action potentials in interneuron dendrites. Science *287*, 295–300.

McCormick, D.A., and Prince, D.A. (1986). Acetylcholine induces burst firing in thalamic reticular neurones by activating a potassium conductance. Nature *319*, 402–405.

McCormick, D.A., and Pape, H.C. (1988). Acetylcholine inhibits identified interneurons in the cat lateral geniculate nucleus. Nature *334*, 246–248.

Montero, V.M. (1986). Localization of gamma-aminobutyric acid (GABA) in type 3 cells and demonstration of their source to F2 terminals in the cat lateral geniculate nucleus: a Golgi-electron-microscopic GABA-immunocytochemical study. J. Comp. Neurol. *254*, 228–245.

Murphy, G.J., Darcy, D.P., and Isaacson, J.S. (2005). Intraglomerular inhibition: signaling mechanisms of an olfactory microcircuit. Nat. Neurosci. *8*, 354–364.

Norton, T.T., and Godwin, D.W. (1992). Inhibitory GABAergic control of visual signals at the lateral geniculate nucleus. Prog. Brain Res. *90*, 193–217.

Norton, T.T., Holdefer, R.N., and Godwin, D.W. (1989). Effects of bicuculline on receptive field center sensitivity of relay cells in the lateral geniculate nucleus. Brain Res. *488*, 348–352.

Pape, H.C., and McCormick, D.A. (1995). Electrophysiological and pharmacological properties of interneurons in the cat dorsal lateral geniculate nucleus. Neuroscience *68*, 1105–1125.

Pouille, F., and Scanziani, M. (2001). Enforcement of temporal fidelity in pyramidal cells by somatic feed-forward inhibition. Science *293*, 1159–1163.

Pouille, F., and Scanziani, M. (2004). Routing of spike series by dynamic circuits in the hippocampus. Nature *429*, 717–723.

Rafols, J.A., and Valverde, F. (1973). The structure of the dorsal lateral geniculate nucleus in the mouse. A Golgi and electron microscopic study. J. Comp. Neurol. *150*, 303–332.

Ralston, H.J., 3rd. (1971). Evidence for presynaptic dendrites and a proposal for their mechanism of action. Nature *230*, 585–587.

Schiller, J., Major, G., Koester, H.J., and Schiller, Y. (2000). NMDA spikes in basal dendrites of cortical pyramidal neurons. Nature *404*, 285–289.

Schneggenburger, R., and Neher, E. (2005). Presynaptic calcium and control of vesicle fusion. Curr. Opin. Neurobiol. *15*, 266–274.

Sherman, S.M. (2004). Interneurons and triadic circuitry of the thalamus. Trends Neurosci. *27*, 670–675.

Silberberg, G., and Markram, H. (2007). Disynaptic inhibition between neocortical pyramidal cells mediated by Martinotti cells. Neuron *53*, 735–746.

Sillito, A.M., and Kemp, J.A. (1983). The influence of GABAergic inhibitory processes on the receptive field structure of X and Y cells in cat dorsal lateral geniculate nucleus (dLGN). Brain Res. *277*, 63–77.

Svoboda, K., and Yasuda, R. (2006). Principles of two-photon excitation microscopy and its applications to neuroscience. Neuron *50*, 823–839.

Tamamaki, N., Yanagawa, Y., Tomioka, R., Miyazaki, J., Obata, K., and Kaneko, T. (2003). Green fluorescent protein expression and colocalization with calretinin, parvalbumin, and somatostatin in the GAD67-GFP knock-in mouse. J. Comp. Neurol. *467*, 60–79.

Usrey, W.M., and Reid, R.C. (1999). Synchronous activity in the visual system. Annu. Rev. Physiol. *61*, 435–456.

Waters, J., Schaefer, A., and Sakmann, B. (2005). Backpropagating action potentials in neurones: measurement, mechanisms and potential functions. Prog. Biophys. Mol. Biol. *87*, 145–170.

Wei, D.S., Mei, Y.A., Bagal, A., Kao, J.P., Thompson, S.M., and Tang, C.M. (2001). Compartmentalized and binary behavior of terminal dendrites in hippocampal pyramidal neurons. Science *293*, 2272–2275.

Xiong, W., and Chen, W.R. (2002). Dynamic gating of spike propagation in the mitral cell lateral dendrites. Neuron *34*, 115–126.

Xu, W., and Lipscombe, D. (2001). Neuronal Ca(V)1.3alpha(1) L-type channels activate at relatively hyperpolarized membrane potentials and are incompletely inhibited by dihydropyridines. J. Neurosci. *21*, 5944–5951.

Zelles, T., Boyd, J.D., Hardy, A.B., and Delaney, K.R. (2006). Branch-specific Ca2+ influx from Na+-dependent dendritic spikes in olfactory granule cells. J. Neurosci. *26*, 30–40.

Zhu, J.J., Uhlrich, D.J., and Lytton, W.W. (1999). Burst firing in identified rat geniculate interneurons. Neuroscience *91*, 1445–1460.

Zucker, R.S., and Regehr, W.G. (2002). Short-term synaptic plasticity. Annu. Rev. Physiol. *64*, 355–405.